Electronic Supplementary Information

Light-Confining Semiconductor Nanoporous Anodic Alumina Optical Microcavities for Photocatalysis

Lina Liu[1,2,6], Siew Yee Lim[2,3,4], Cheryl Suwen Law[2,3,4], Bo Jin[2], Andrew D. Abell[*3,4,5], Gang Ni[1,6] and Abel Santos[*2,3,4]

[1]State Key Laboratory of High-efficiency Utilization of Coal and Green Chemical Engineering, Ningxia University, Yinchuan 750021, P.R. China.
[2]School of Chemical Engineering and Advanced Materials, The University of Adelaide, Adelaide, South Australia 5005, Australia.
[3]Institute for Photonics and Advanced Sensing, The University of Adelaide, Adelaide, South Australia 5005, Australia.
[4]ARC Centre of Excellence for Nanoscale BioPhotonics, The University of Adelaide, Adelaide, South Australia 5005, Australia.
[5]Department of Chemistry, The University of Adelaide, Adelaide, South Australia 5005 Adelaide, Australia.
[6]College of Chemistry and Chemical Engineering, Ningxia University, Yinchuan 750021, P. R. China.

***E-Mails:** andrew.abell@adelaide.edu.au ; abel.santos@adelaide.edu.au

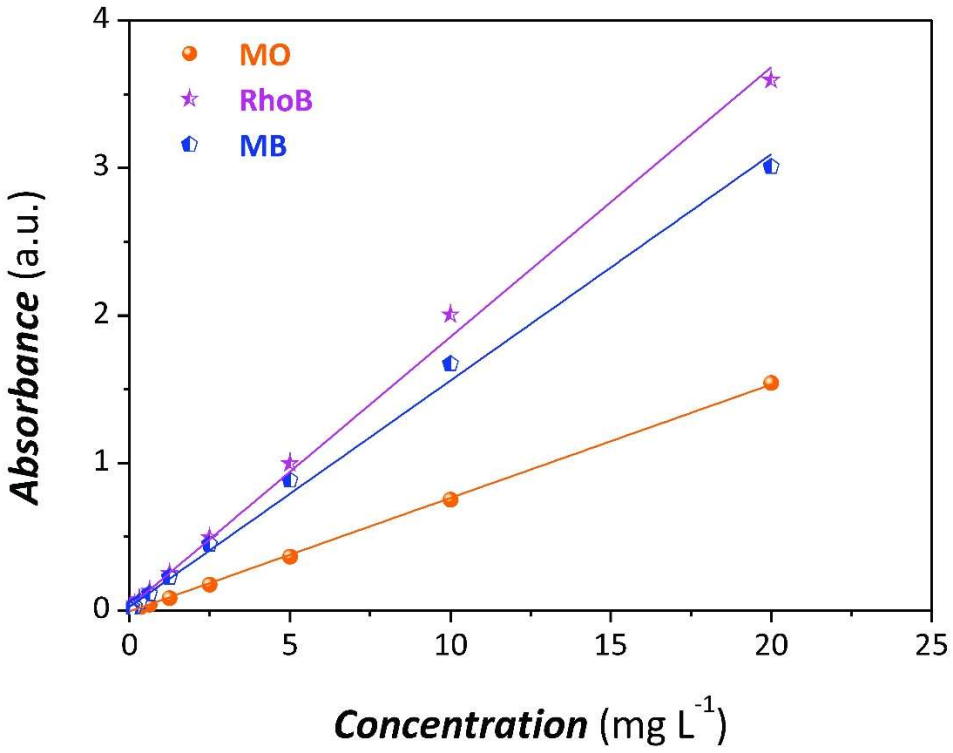

Figure S1. Linear correlation between absorbance and concentration of methylene blue (MB), rhodamine B (RhoB), and methyl orange (MO) (NB: concentration range from 0.00244 to 10 mg L^{-1}). The linear correlation for MB, RhoB and MO were: Abs_{MB} (a.u.) = 0.1697 *[MB]* (mg L^{-1}), Abs_{RhoB} (a.u.) = 0.19998 *[RhoB]* (mg L^{-1}) and Abs_{MO} (a.u.) = 0.07436 *[MO]* (mg L^{-1}), respectively. The R^2 values for MB, RhoB and MO were 0.99923, 0.99979, and 0.99940, respectively.

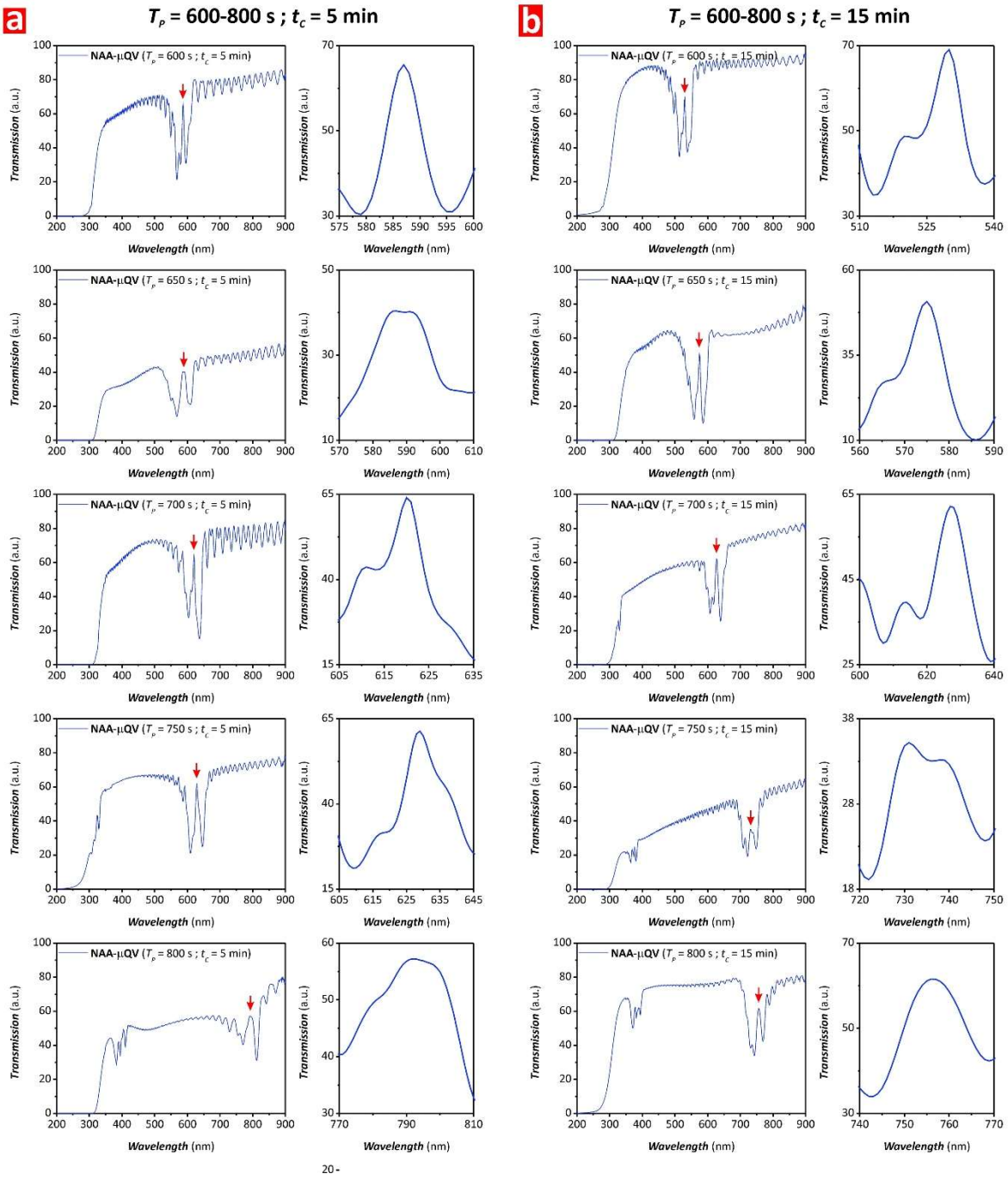

Figure S2. Transmission spectra of NAA-µQVs produced with T_P = 600–800 s and a) t_C = 5 min (a) and t_C = 15 min (b) (NB: full range spectra with red arrows indicating the position of the resonance band (left) and magnified view of resonance band (right)).

Table S1. Optical features (i.e. resonance intensity – I_R, resonance central wavelength – λ_R, full width at half maximum – $FWHM_R$, and quality factor – Q_R) of NAA-μQVs produced with T_P = 600–800 s and t_C = 5 and 15 min, in air and water.

T_P (s)	t_C (min)	Medium	I_R (a.u.)	λ_R (nm)	$FWHM_R$ (nm)	Q_R
600	5	air	40	587	10	58
	15	air	27	529	9	59
	5	water	16	618	10	64
	15	water	13	537	7	79
650	5	air	27	589	19	31
	15	air	34	569	19	30
	5	water	6	608	16	37
	15	water	9	600	49	12
700	5	air	40	618	18	34
	15	air	36	627	11	57
	5	water	12	687	26	26
	15	water	25	668	10	64
750	5	air	35	630	16	38
	15	air	16	735	17	44
	5	water	31	662	30	21
	15	water	22	785	11	69
800	5	air	39	795	23	35
	15	air	26	14	757	54
	5	water	7	832	27	30
	15	water	27	17	792	48

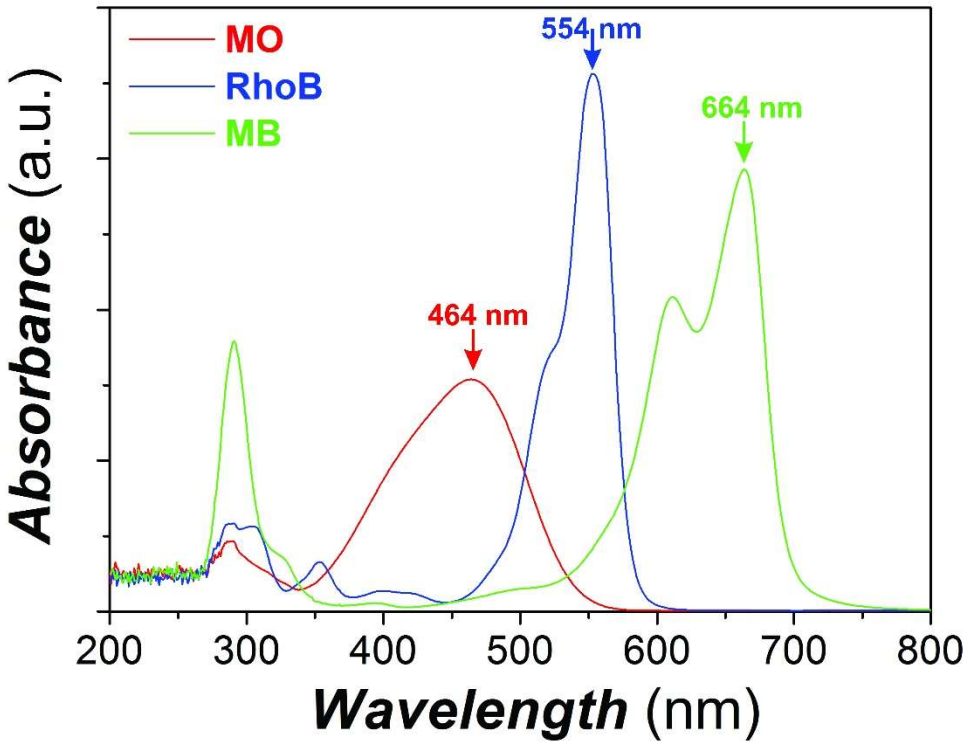

Figure S3. Optical absorbance spectra of methylene blue (MB), rhodamine B (RhoB), and methyl orange (MO). The absorption band maxima for MB, RhoB and MO were and $\lambda_{abs\text{-}MB}$ = 664 nm, $\lambda_{abs\text{-}RhoB}$ = 554 nm, $\lambda_{abs\text{-}MO}$ =464 nm, respectively (NB: the absolute absorption intensities of MB, RhoB and MO at the central position were ~2.8, 3.6 and 1.5 a.u., respectively).

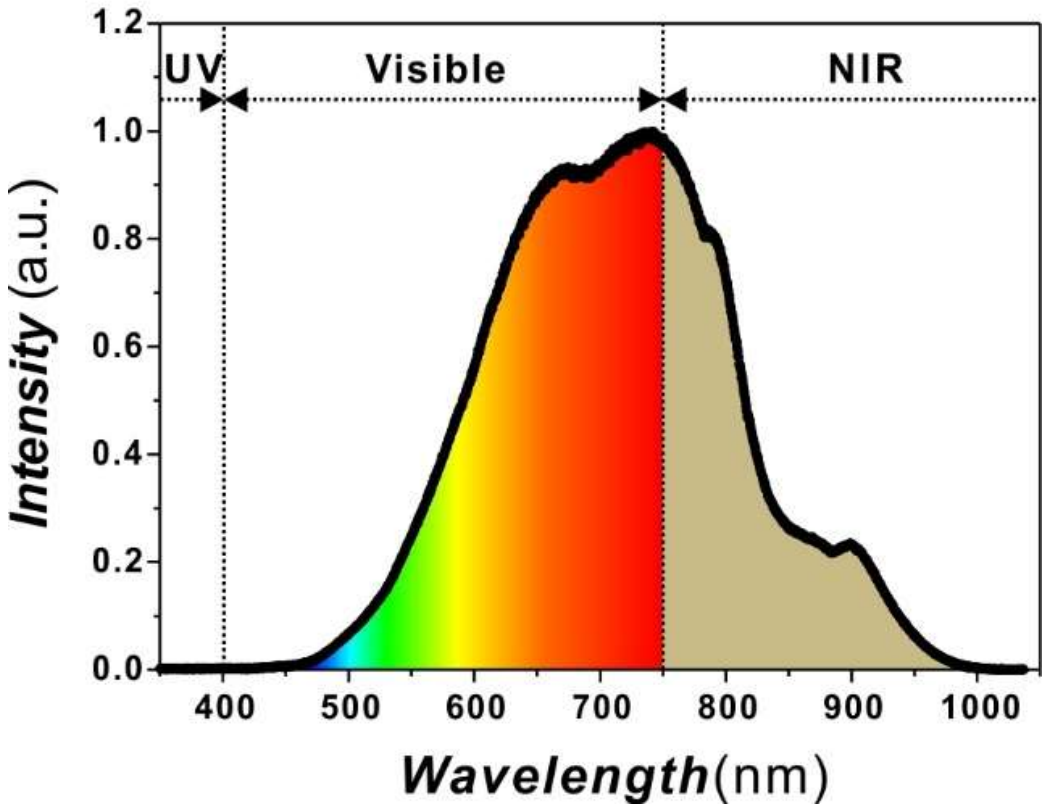

Figure S4. Simulated visible–NIR light irradiation source used for photocatalysis in our study (i.e. 0.12% UV (350–400 nm), 64.60% visible (400–750 nm), and 35.28% NIR (800–1025 nm)). The irradiation spectrum was measured using an optical fiber spectrometer (USB 4000, Ocean Optics, USA).

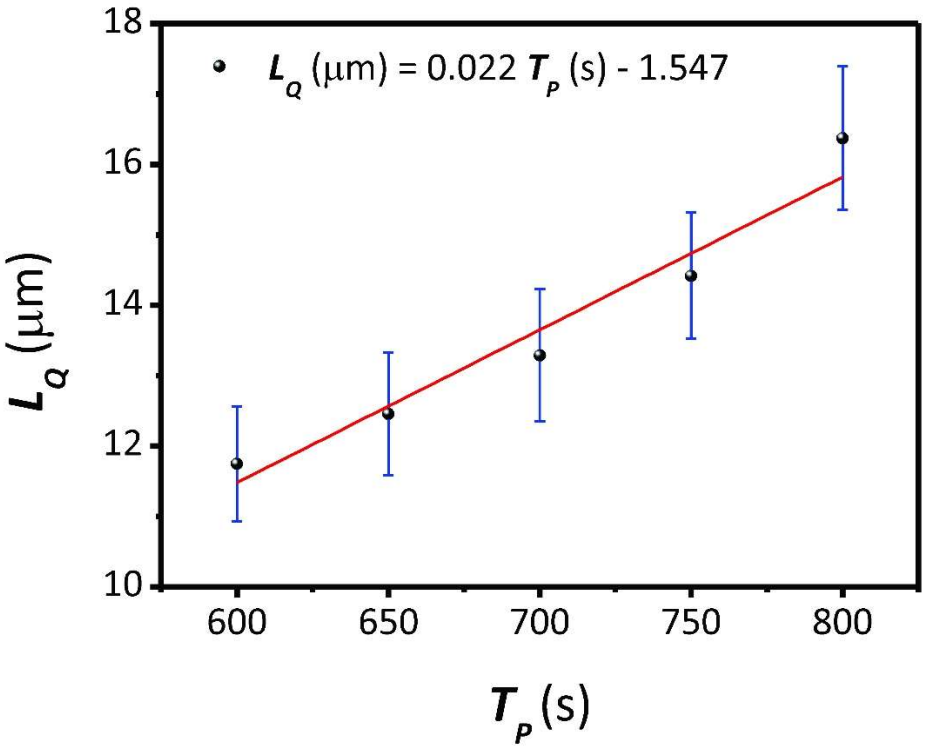

Figure S5. Linear fitting describing the dependence between the total thickness of TiO_2-NAA-μQVs (L_Q) and the anodization period (T_P).

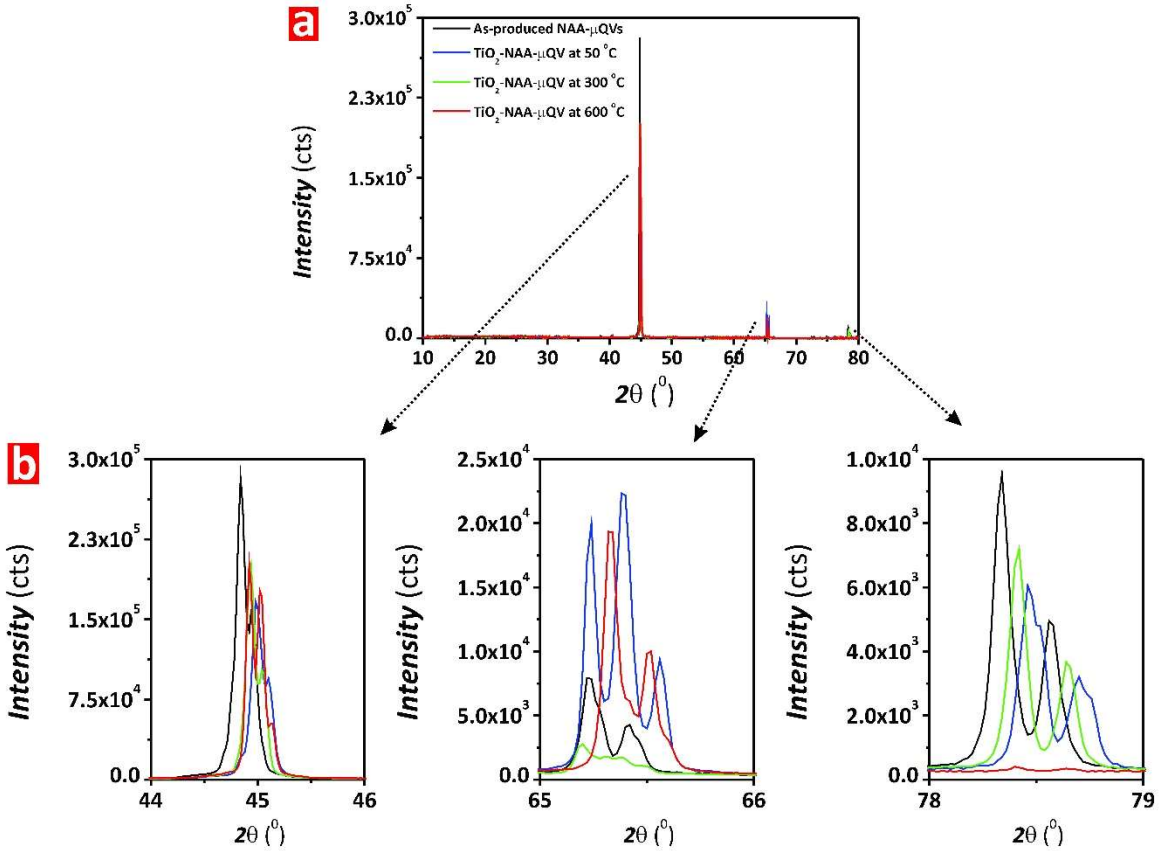

Figure S6. X-ray diffraction (XRD) spectra of a representative NAA-μQVs before and after sol-gel deposition of TiO_2 at different annealing temperatures (50, 300 and 600 °C) (measurements performed in an XRD Rigaku MiniFlex 600). a) General XRD spectrum and b) magnified view of characteristic XRD peaks. NB: Before sol-gel deposition, there are three characteristic peaks in the XRD spectrum located at 45, 65.2 and 78.4°, which correspond to amorphous alumina (Al_2O_3) phase. After deposition of the TiO_2 functional layer, there no additional peak is observed in the XRD spectrum, indicating that the TiO_2 layer is crystallographically amorphous. However, the position of these peaks undergoes a slight shift in their position and their intensity changes, confirming the successful deposition of photo-active layers of TiO_2 onto the inner surface of NAA-μQVs. The crystallographic phase of TiO_2 undergoes transformation from amorphous (50 °C) to rutile (600 °C) phases.